Journal of Molecular Structure 1275 (2023) 134599

Contents lists available at ScienceDirect

Journal of Molecular Structure

journal homepage: www.elsevier.com/locate/molstr

Characterization of hitherto unknown Valsartan photodegradation impurities

Timon Kurzawa[a,*], Salim Fazzani[a], René Tempel[a], Hannes Helmboldt[a], Christian Bleschke[a], Andreas Kohlmann[a], Adelheid Hagenbach[b]

[a] LGC GmbH, Louis-Pasteur-Str. 30, Luckenwalde 14943, Germany
[b] Freie Universität Berlin, Institut für Chemie und Biochemie, Fabeckstr. 34-36, Berlin 14195, Germany

ARTICLE INFO

Article history:
Received 25 August 2022
Revised 9 November 2022
Accepted 19 November 2022
Available online 22 November 2022

Keywords:
Valsartan
Photodegradation
Potential impurities

ABSTRACT

A detailed investigation of Valsartan's light-induced degradation is reported. Based on UPLC-HRMS studies of stressed solutions several degradation pathways are proposed. Some of the proposed structures were obtained by forced degradation experiments. Examination of analytical data including crystal structures allowed for structural revision of one literature-known degradant. In addition, irradiation under aerobic conditions revealed further degradative pathways leading to two previously unknown decomposition products. Mechanistic considerations regarding their origin helped to identify structural weak points of Valsartan under the influence of light.

1. Introduction

Degradation of chemical compounds is an omnipresent and fundamental process in nature. While degradation of small amounts of chemical entities is an unproblematic side effect in many chemical and biological systems, it's occurrence in pharmaceutical products possess the potential to cause serious health risks for patients [1]. Identification, characterization, and mechanistic rationale of possible degradation products are therefore of particular value for safer pharmaceutical substances. As part of the risk minimization for patients, legal authorities demand testing of pharmaceutical products for potential degradation upon external stress. Testing parameters include exposure to heat, light, acidic, basic and oxidative conditions and are defined in the ICH Guidelines Q1A (stability testing of new drug substances and products) [2]. Furthermore, the availability of isolated impurity samples as reference standards is important for exclusion of possible contamination in pharmaceutical products. By testing every batch of API (active pharmaceutical ingredient) for potential impurities prior to release the highest possible safety standards are maintained.

In this account, we wish to report our results from light-induced degradation studies of Valsartan **1** (Fig. 1). Valsartan is a Top200 drug that is used as orally administrable angiotensin II (AT_1)-antagonist for treatment of hypertension, diabetic nephropathy, and congestive heart failure [3,4]. For sartans, degradation pathways are of particular interest due to recent *N*-nitrosodimethylamine impurity-related retractions of large amounts of formulated products in Europe and the US market [5].

Several other groups have already studied Valsartan degradation processes under irradiation with overall mixed results. Some reports described Valsartan as photostable [6–8] under conditions according to ICH Guidelines Q1B (photostability testing of APIs) [9]. Others observed degradation without structure determination of the decomposed compounds [10–12]. Bianchini et al. isolated decarboxylated Valsartan **2** and diazirine compound **3**. Diazirine **3** results from cyclization of the tetrazole moiety and biphenyl towards phenanthridines with simultaneous ring diminishment (Fig. 1) [13,14]. Mehta et al. proposed similar diazirine structures during mass spectrometric studies as part of the fragmentation pattern of cyclized compound **4**. However, no attempts to isolate such species were undertaken [15]. In addition, phenanthridine **4** was obtained by Kumaraswamy et al. by refluxing of **1** under basic conditions [16]. Light-induced cyclization of Valsartan **1** towards phenanthridine cores is a plausible degradation pathway due to the close proximity of tetrazole and biphenyl moiety. In addition, the conjugated system is significantly increased through planarization. A ring contraction under release of nitrogen on the other hand seems unlikely, given the missing precedence in the literature for this kind of transformation under ambient conditions [17–19] and the general instability reported for diazirines [20,21].

* Corresponding author.
E-mail address: timon.kurzawa@lgcgroup.com (T. Kurzawa).

https://doi.org/10.1016/j.molstruc.2022.134599

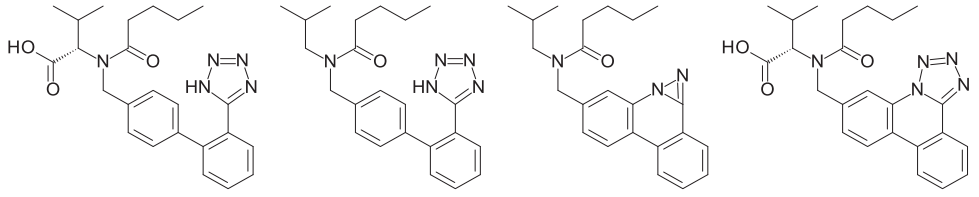

Fig. 1. Valsartan and selected literature-known degradation products.

We were therefore particularly interested in the investigation of diazirine containing structures, because their formation might cause serious side effects in the pharmaceutical application due to their anticipated instability.

2. Experimental section

2.1. Chemicals and materials

Valsartan was purchased from Afine Chemicals Limited. MeCN, H_2O, EtOAc, CH_2Cl_2, *n*-hexane and MeOH (all HPLC-grade) and *t*BuOH (reagent grade) were purchased from VWR International GmbH and were used without further purification.

2.2. Instrumentation

Chromatographic separations were performed using Isolera Four® from Biotage and mixtures of *n*-hexane/EtOAc for normal phase chromatography (column material: silica gel) and H_2O/MeCN for reverse phase (column material: YMC ODSAQ C18-S 12 nm). NMR spectra were measured in $CDCl_3$ (for compounds **2, 5** and **6**) and DMSO-d_6 (compound **10**) on a Bruker Avance Neo 400. Tetramethyl silane was used as internal standard. FT-IR measurements were performed using a Jasco FT/IR 4100. Melting points were measured on a Mettler-Toledo MP90. HRMS measurements were carried out on a Thermo Scientific Exactive Plus. CHN analysis was performed on a Elementar Vario EL Cube. UPLC-MS measurements were conducted on a Waters UPLC Acquity H Class with Acquity QDa and Acquity PDA eλ detector using a Waters Acquity UPLC HSS T3 column (1.8µm; 2.1 × 100 mm). H_2O + 0.1% formic acid (A) and acetonitrile (B) were used as eluents at 40 °C and a flow rate of 0.5 mL/min. A gradient of 0 min 90% A 10% B, 0.1 min 90% A 10% B, 12 min 20% A 80% B, 13 min 2% A 98% B, 15 min 90% A 10% B, 19 min 90% A 10% B was applied. Mass spectra were obtained in a range of 100–600 amu, with a cone voltage of 15 V and a capillary voltage of 0.8 kV at 600 °C. UV-Vis spectra were analyzed based on a wavelength of 200 nm to prevent overestimation of phenanthridine percentage. A comparison at 225 nm (pharmacopeial wavelength for **1**) gave higher percentages for the phenanthridine compounds (see supporting information for comparison). UPLC-HRMS measurements were performed on a Dionex UltiMate 3000 using a Waters Cortecs UPLC column (1.6µm; 2.1 × 75 mm). H_2O + 0.1% formic acid (A) and acetonitrile + 0.1% formic acid (B) were used as eluents at 40 °C and a flow rate of 0.5 mL/min. A gradient of 0 min 98% A 2% B, 3 min 2% A 98% B, 4 min 2% A 98% B, 5 min 98% A 2% B, 6 min 98% A 2% B was applied. Mass spectra were obtained in a range of 80.0–1000.0 amu, with capillary voltage of 3.5 kV at 269 °C. For X-ray structure determination intensities were collected on a BRUKER D8 Venture system (compound **5**) and STOE IPDS II instruments with Mo Kα radiation (compound **6**). Space groups were determined by detection of systematical absences. Structure solution and refinement were performed using the SHELX program package [22,23]. Hydrogen atoms were treated with the "riding model" option of SHELXL. Molecular structures were visualized using DIAMOND 4.2.2 [24]. For further information see supporting information.

2.3. Photostability studies

Method A: Solutions of Valsartan in MeCN (1.0 mg/mL) were irradiated at 20 °C in the presence of oxygen for 4 h using a 150 W Hg medium pressure UV light source in a photo cabinet purchased from Peschl Ultraviolet. Pyrex equipment was used in order to eliminate any irradiation λ <320 nm according to conditions described in the ICH Q1B guidelines [9]. The UV-A radiant output was 5.40 mW/cm^2 at a distance of 8.5 cm. The degradation of Valsartan was monitored by UPLC-MS. The identity of the degradation products was ensured by co-injection with isolated compounds obtained via forced degradation (2.4).

Method B: Solutions of Valsartan in MeCN (1.0 mg/mL) were left standing in the sun at 25 °C for 1 d (approximately 15 h of sunlight) in Pyrex vials. The degradation of Valsartan was monitored by UPLC-MS and UPLC-HRMS. The identity of the degradation products was ensured by co-injection with isolated compounds obtained via forced degradation (2.4).

2.4. Forced degradation for structure determination

Forced degradation studies were performed in the presence and absence of oxygen using a 150 W Hg medium pressure UV light source in a photo cabinet purchased from Peschl Ultraviolet. According to the procedure of Bianchini et al. [13,14], Valsartan **1** (3.0 g, 6.9 mmol) was dissolved in *t*BuOH/H_2O (600 mL, 1:2) and was irradiated at rt for up to 2 d. Alternatively, MeCN was used as solvent. Both Pyrex and quartz glass equipment was tested, with the latter giving generally faster conversion. After irradiation, product mixtures were concentrated under reduced pressure and purified by normal phase chromatography (*n*-hexan/EtOAc, 18 column volumes (CV) 5–100% B, 2 CV 100% B). Product fractions with a purity (by UPLC) of >90% were pooled and purified by reverse phase chromatography (H_2O/MeCN, 1 CV 0% B, 10 CV 0–100% B, 4 CV 100% B). If neccessary, these operations were repeated until sufficiently pure material for structure elucidation of compounds **2, 5, 6** and **10** was obtained. Then, products were crystallized from *n*-hexane (**2**, purity by UPLC: 99.80%), CH_2Cl_2 (**5** and **6**, purity: 98.82% and 96.62%) or MeOH (**10**, purity: 97.38%).

3. Results and discussion

3.1. Photostability studies

As already observed by Bianchini et al. [13,14], Mehta et al. [15] and Kumaraswamy et al. [16], stressing Valsartan under exclusion of irradiation λ <320 nm using conditions in line with ICH Q1B [9] (method A) gave several degradation products within 4 h in relevant levels (>0.1%, see supporting information for details). When Valsartan was left standing in the sun in solution

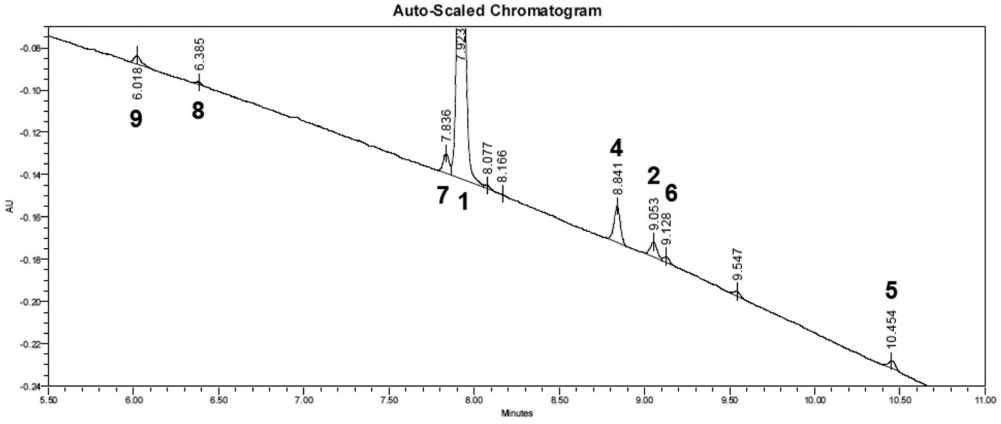

Fig. 2. UPLC chromatogram of Valsartan in MeCN (0.1 mg/mL) left in the sun for 1 d (Method B, see supporting information for full chromatogram).

Table 1
Retention time, HRMS and Area% of impurities formed during stability studies.

	rt [min]	compound	composition	calc. $[M+H]^+$	found $[M+H]^+$	Δ [ppm]	Area%[a] Method A	Area%[a] Method B
1	7.92	1 (API)	$C_{24}H_{30}N_5O_3$	436.23432	436.23470	0.9	88.91	90.03
2	9.04	2	$C_{23}H_{30}N_5O$	392.24449	392.24463	0.4	4.92	2.49
3	–	3	$C_{23}H_{28}N_3O$	362.22269	–	–	Not observed	Not observed
4	8.84	4	$C_{24}H_{28}N_5O_3$	434.21867	434.21901	0.8	0.28	1.57
5	10.45	5	$C_{23}H_{28}N_5O$	390.22884	390.22859	0.6	0.40	0.44
6	9.12	6	$C_{20}H_{20}N_5O_2$	362.16115	362.16114	0.0	0.13	0.23
7	7.83	7	$C_{20}H_{22}N_5O_2$	364.17680	364.17681	0.0	3.31	2.13
8	6.38	8	$C_{19}H_{22}N_5O$	336.18189	336.18171	0.5	Not observed[b]	0.35
9	6.02	9	$C_{13}H_{11}N_4$	223.09782	223.09789	0.3	Not observed[b]	0.77
			Total decomposition (including unidentified degradants):				11.10	9.97

[a] Average of two runs with two independently stressed samples.
[b] Formation of compounds **8** and **9** was only observed in sunlight-stressed samples (Method B). Overall, decarboxylation of **1** seems to proceed faster under artificial light conditions (Method A) than under the influence of sunlight (Method B).

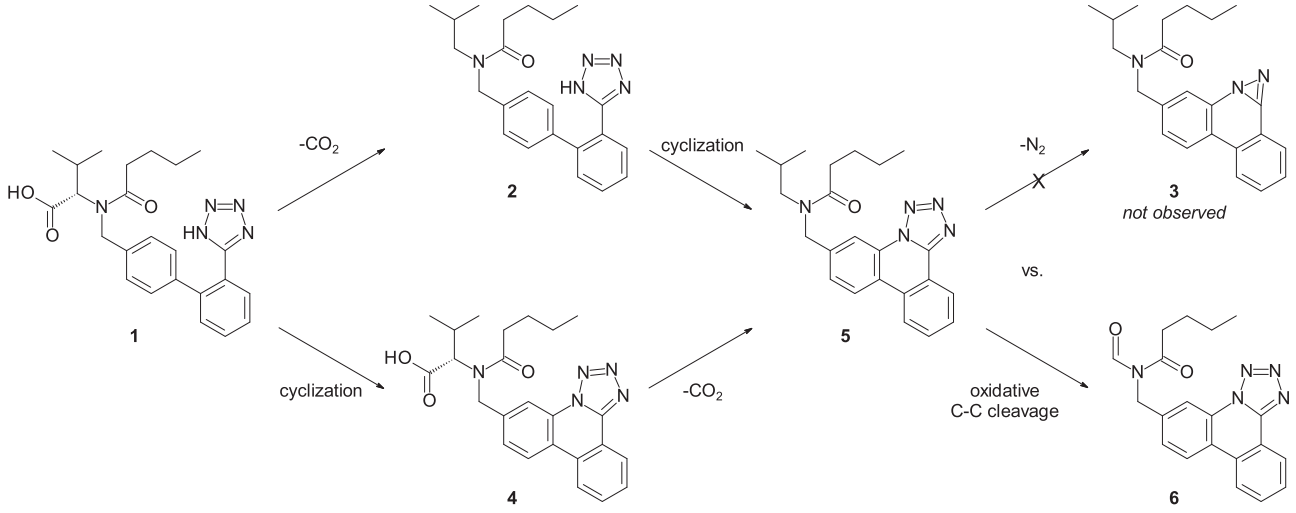

Scheme 1. Structural proposals for cyclization derived degradation products based on UPLC-HRMS results.

for 1 d, comparable amounts of the same degradants were observed (method B, Fig. 2, Table 1). Based on UPLC-MS and UPLC-HRMS data (see supporting information for details) some degradative pathways and resulting structures can be proposed (Schemes 1 and 2). A decarboxylation of Valsartan **1** furnishes literature known compound **2** [13,14] (Scheme 1). A cyclization event results in phenanthridine **4**, as described by Mehta et al. [15] and Kumaraswamy et al. [16], a subsequent decarboxylation gives phenanthridine **5**. A diazirine formation under exclusion of N_2 would result in degradation product **3**, however, no matching mass was observed. An oxidative formamide formation under degradation of the valine subunit gives compound **6**. For proposed structures **2** and **4** matching masses were also observed in negative electrospray ionization (ESI) mode. For proposed cyclized structures **4, 5** and **6** a characteristic shift of the UV maxima was observed. This is plausible due to the significant extension of the chromophore's conjugation.

Structure proposals for non-cyclized degradation products are given in Scheme 2. In analogy to formation of formamide **6**, an oxidative degradation of the valine subunit would give degradation product **7**. A disconnection within the valine results in amide **8**, as described by Mehta et al. [15]. The mass of a diphenyl tetrazole

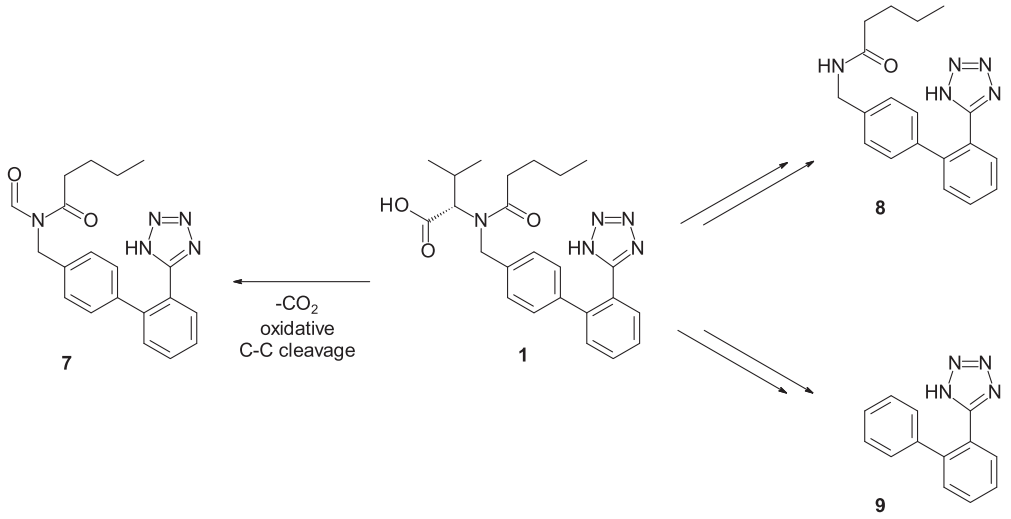

Scheme 2. Structural proposals for non-cyclized photodegradation products based on UPLC-HRMS results.

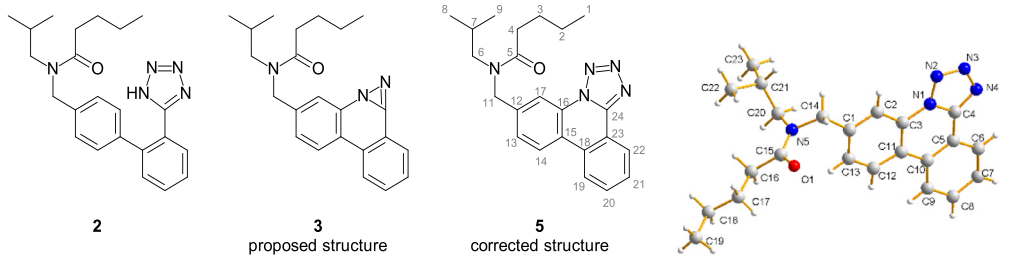

Fig. 3. Decarboxylated Valsartan **2**, proposed structure **3**, corrected structure **5** and its X-ray.

fragment **9** was also detected, although details about its formation remain unclear. For proposed structures **7, 8** and **9** matching masses were also observed in negative ESI mode. The percentage of each impurity formed, the calculated and observed HRMS and total degradation of **1** during photostability study is given in Table 1.

3.2. Forced degradation under oxygen exclusion

In order to produce substantial amounts of these degradation products for structure elucidation, photodegradation of Valsartan was studied under more forcing conditions. During these degradation studies, partially decomposed Valsartan structures **2** and **5** were isolated and identified under anaerobic conditions (Fig. 3). Compound **2** results from decarboxylation of the API and has already been reported by Bianchini et al. [13,14]. Phenanthridine **5** was found to give analytical data which matched diazirine **3** [13,14] in all aspects excluding mass spectrometry (see Table 2 for comparison of NMR data and supporting information for detailed analytical data). Diazirine **3** and tetrazole **5** cannot be distinguished solely based on IR and NMR data interpretation. Further investigation by elemental analysis, HRMS and crystal structure (Fig. 3) confirmed the intact tetrazole unit rather than the previously described diazirine **3**. In addition, UPLC-MS measurements revealed a partial formation of **3** under ESI-MS conditions from pure **5** with increased ionization voltage (see supporting information for details). This observation could explain the assignment of diazirine **3** as structure for **5** by ionization-induced *in situ* ring diminishment during HRMS measurements. Although tetrazole **5** as structure of our cyclization product is sufficiently proven, we cannot fully exclude formation of **3** as reported in the literature. Both products **2** and **5** were confirmed as degradation products by spiking experiments with sunlight-stressed samples (see supporting information for details). Phenanthridine **4** could not be obtained under these conditions since decarboxylation of Valsartan **1** appears to proceed faster than cyclization. However, under basic stress conditions a decarboxylation might be suppressed, as demonstrated by Kumaraswamy et al. under thermic stress [16].

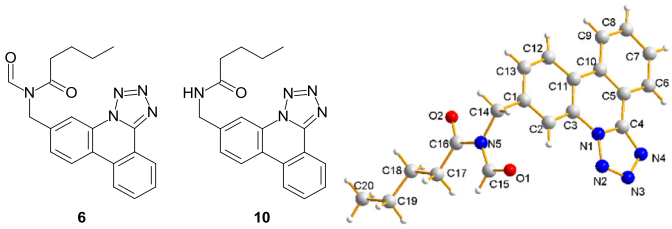

Fig. 4. Structure of degradants **6** and **10** formed in the presence of oxygen and X-ray of **6**.

3.3. Photodegradation in the presence of oxygen

In addition, forced Valsartan degradation in the presence of oxygen was investigated to evaluate the influence of oxygen on the API's degradative pathways. Together with the already observed degradation products **2** and **5**, we isolated and characterized formamide **6** and amide **10** (Fig. 4, see supporting information for 2D-NMR data, structure elucidation and analytical details). The structure of formamide **6** was confirmed via X-ray structure determination. The origin of both compounds lies in the degradation of Valsartan's former valine unit. Oxidative C-C bond cleavage under irradiation at α-position in amines is a common degradation process, which has been extensively studied and supported by theoretical calculations for a variety of substrates [25–27]. Besides, sev-

Table 2
NMR comparison of **3** [13,14] and **5**.

	NMR-data for **5** in $CDCl_3$						NMR-data reported for **3** [13,14] in $CDCl_3$					
	^{1}H [ppm]	**Multiplicity** [Hz]	**Integral**	**APT** [ppm]	**COSY** correlations	**HMBC** correlations	**^{1}H** [ppm]	**Deviation**	**Multiplicity** [Hz]	**^{13}C** [ppm]	**Deviation**	**assigned as**
1	0.89*, 0.98	t, 7.4	3	14.0, 13.9*	1→2	1→2, 1→3	0.97	0.01	t, 7.1	13.9	0	1
2	1.44, 1.34*	tq, 7.5, 7.4	2	22.7, 22.5*	2→1, 2→3	2→1, 2→3, 2→4	1.43	0.01	sextet, 7.7	22.6	0.1	2
3	1.68*, 1.74	tt, 7.5, 7.5	2	27.65, 27.56*	3→2, 3→4	3→1, 3→2, 3→4, 3→5	1.73	0.01	quint, 7.5, 7.5	27.6	0	3
4	2.48, 2.39*	t, 7.5	2	33.3*, 33.0	4→3	4→2, 4→3, 4→5	2.48	0	bdd, 7.6, 7.6	33.0	0	4
5	x	x	x	174.1, 173.8*	x	3→5, 4→5, 11→5	x	x	x	174.1	0	5
6	3.34, 3.21*	d, 7.5	2	55.2, 53.5*	6→7, 6→11	6→5, 6→7, 6→8, 6→9	3.20	0.01	d, 7.5	55.3	0.1	6
7	2.04, 2.06*	qq, 6.7, 6.7	1	27.9, 27.1*	7→8, 7→9, 7→6	7→6, 7→8, 7→9	1.96–2.07	0	m	27.9	0	7
8	0.95*, 0.98	d, 6.7	3	20.2*, 20.1	8→7	8→6, 8→7, 8→9	0.97	0.01	d, 6.7	20.1	0.1	8
9	0.95*, 0.98	d, 6.7	3	20.2*, 20.1	9→7	9→6, 9→7, 9→8	0.97	0.01	d, 6.7	20.1	0.1	9
10	-	-	-	-	-	-	-	-	-	-	-	-
11	4.87, 4.84*	s	2	51.4*, 48.8	11→6, 11→13, 11→17	11→5, 11→6, 11→12, 11→13, 11→17	4.86	0.01	s	48.8	0	11
12	x	x	x	141.3, 140.5*	x	14→12	x	x	x	141.3	0	12
13	7.64, 7.53*	dd, 8.5, 1.7	1	127.8, 125.8*	13→11, 13→14, 13→17	13→11, 13→14, 13→15, 13→17	7.68	0.04	d, 7.8	127.8	0	19
14	8.52–8.43	m	1	124.8*, 124.4	14→13	14→12, 14→15, 14→16	8.54–8.40	0	m	124.3	0.1	21
15	x	x	x	121.7*, 121.3	x	13→15, 14→15, 17→15	x	x	x	118.5[a]	0	15
16	x	x	x	129.8	x	14→16, 17→16	x	x	x	129.8[a]	0	23
17	8.52–8.43	m	1	116.0, 115.3*	17→11	17→11, 17→13, 17→18	8.54–8.40	0	m	123.0[a]	-	17
18	x	x	x	129.4	x	19→18, 20→18, 22→18	x	x	x	125.8[a]	-	18
19	8.52–8.43	m	1	123.03*, 122.95	19→20, 19→21	19→18, 19→20, 19→21, 19→23	8.45	0	d, 1.5	123.0[a]	0	17
20	7.91*, 7.88	td, 7.4, 0.7	1	132.1*, 132.0	20→19, 20→20, 20→22	20→18, 20→21, 20→22	7.88	0	d, 7.2	131.9[a]	0.1	22
21	7.80*, 7.78	dt, 7.1, 1.0	1	129.5*, 129.2	21→19, 21→20, 21→22	21→19, 21→22, 21→23	7.77	0.01	d, 7.8	129.2[a]	0	13
22	8.75, 8.77*	dd, 7.9, 0.84	1	126.2*, 126.1	22→20, 22→21	22→21, 22→23, 22→24	8.75	0	dd, 7.8, 1.5	126.1[a]	0	14
23	x	x	x	118.6*, 118.5	x	19→23, 21→23	x	x	x	118.5[a]	0	15
24	x	x	x	147.4*, 147.3	x	22→24	x	x	x	147.3	0	24

3:1 mixture of rotamers, * marks signals of the minor rotamer. For **3**, a similar mixture was described, but only signals of the major rotamer were reported. The published NMR data includes some incorrect assignments (13-H, 14-H, 19-H, 20-H, 21-H, 22-H, C13-C23). The corrected NMR data for **5** was assigned based on 2D NMR data (^{1}H, APT, COSY, HSQC, HMBC) and comparison with **6** and **10**, for which no mixture of rotamers was observed.

[a] For details concerning the corrected structure assignment of NMR data see supporting information.

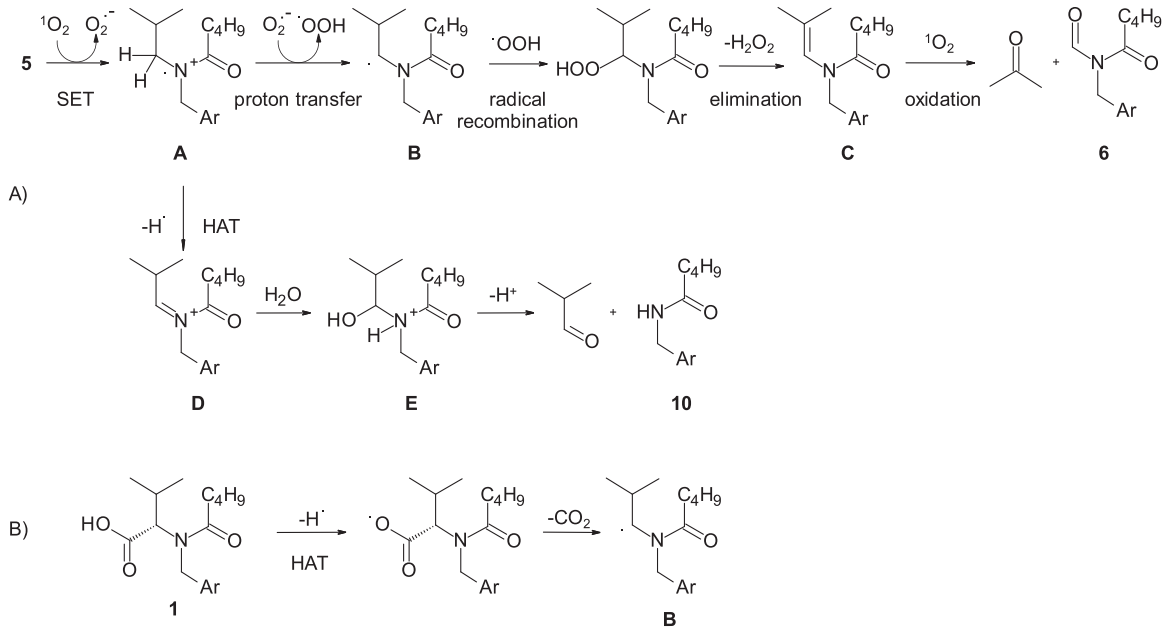

Scheme 3. Mechanistic hypothesis for formation of formamide **6** and amide **10**.

eral chemical methods for this kind of transformation have been reported which use transition metal catalysts in combination with oxidants [28–32] or metal free conditions [33–34]. Mechanistically formamide formation is described as radical-based process in most of these cases, which is also likely to be the modus operandi for Valsartan photodegradation. We propose the following degradative pathways (Scheme 3a) in analogy to literature known methodology [25]. Due to the already mentioned shift in the phenanthridine moiety's UV spectra (see supporting information for full spectra), phenanthridine **5** should be able to act as a photosensitizer, which upon relaxation converts $^3O_2$ to $^1O_2$ via intersystem crossing. This highly reactive species is believed to oxidize **5** to the radical cation **A** via single electron transfer (SET) under formation of $O_2^{\cdot-}$. Radical cation **A** could then undergo a proton transfer, which generates a radical in alpha position to the amine (**B**). A recombination with a hydroperoxyl radical would then deliver the enamine **C** after elimination of H_2O_2. A formal 1,2-addition/oxidative cleavage sequence with $^1O_2$ would furnish formamide **6** and acetone. The presence

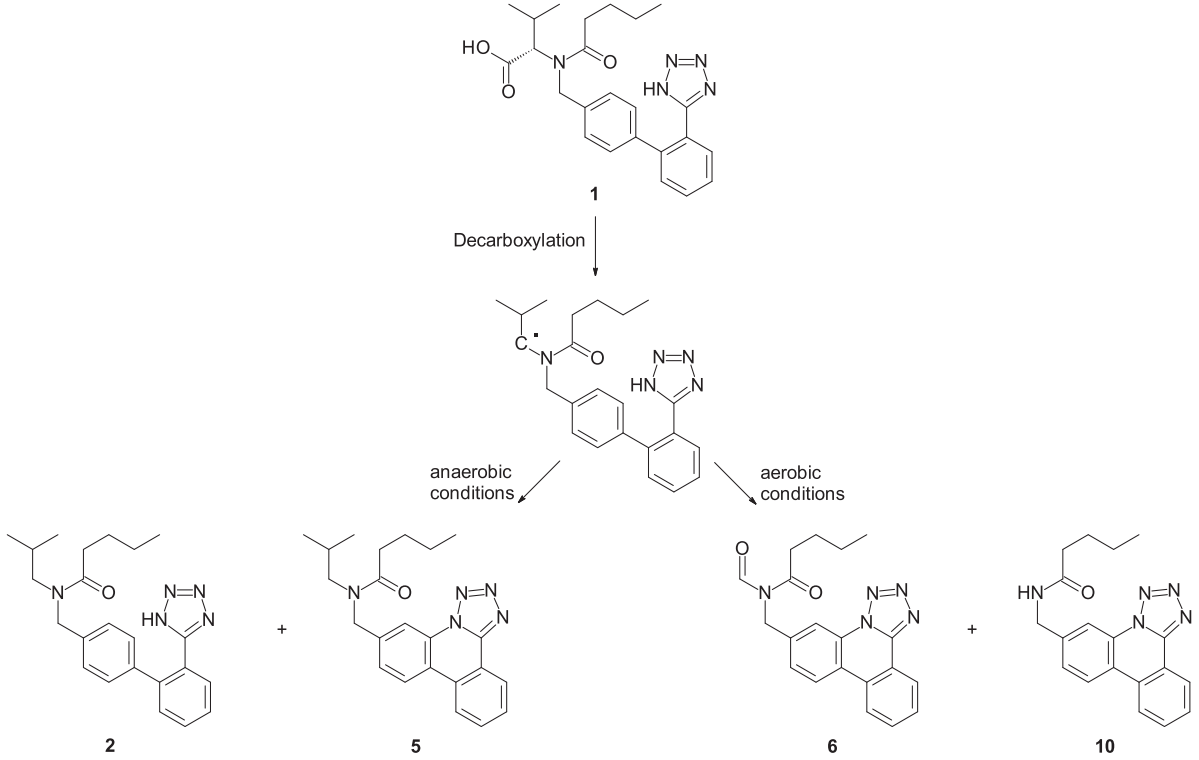

Scheme 4. Proposed light-induced degradation pathways of Valsartan under forced degradation conditions.

of H_2O_2 or other peroxo-species in the stressed Valsartan solution was documented by peroxide tests (Merckoquant®, KI starch paper). On the other hand, the oxidized radical cation **A** could form an iminium ion **D** via hydrogen atom transfer (HAT). The addition of H_2O would result in hemiaminal **E** formation, which furnishes amide **10** and isobutyl aldehyde after deprotonation (Scheme 3a). We speculate that for Valsartan, oxidative valine degradation is facilitated by radical formation adjacent to the amine (**B**) during decarboxylation of **1** (Scheme 3b). While quenching the radical under anaerobic conditions leads to decarboxylated products **2** and **5**, formamide **6** is predominantly formed in the presence of oxygen. Formamide **6** was secured as degradation product by spiking experiments with the sunlight-stressed sample (see supporting information for details). Non-cyclized products **7** and **8** could not be obtained since cyclization seems to proceed faster than oxidative valine degradation under forced degradation conditions. Nevertheless, isolation of amide **10** hints at formation of amide **8** to represent a serious degradation pathway for Valsartan.

4. Conclusion

Based on our results, we propose the following degradative processes (Scheme 4). Decarboxylation of Valsartan is the fastest degradative process under forced light induced degradation conditions, followed by cyclization. The nature of the valine fragment's degradation pathway is highly dependent on the presence of oxygen. While under exclusion of oxygen products containing isobutyl residues are obtained, under aerobic conditions further isobutyl chain degradation was observed to deliver formamide **6** and amide **10**. Ring diminishment of the tetrazole unit was not observed in any case as judged by UPLC-HRMS results and analytical data of isolated material.

In summary, we report the isolation and characterization of three previously unknown Valsartan degradation products **5, 6** and **10**. Structural elucidation based on 2D-NMR, UPLC-MS, elemental analysis, and X-ray analysis suggests the misassignment of **3** in the literature. Mechanistic explanation for the formation of two previously unknown irradiation-derived products **6** and **10** is proposed. In combination, these results give a better insight into light-induced degradation pathways of Valsartan.

During our degradation studies, we identified the valine subunit and the combination of the biphenyl/tetrazole ring system as Valsartan's structural weak points under the influence of light. In particular, degradation of the valine by decarboxylation and oxidative C-C cleavage was observed to furnish several impurities, together with cyclization towards phenanthridines. Given the sartans' structural similarities, the formation of equivalent phenanthridine impurities for other compounds of this class is likely and will be the subject of future investigation.

Declaration of Competing Interest

The authors declare the following financial interests/personal relationships which may be considered as potential competing interests:

T. Kurzawa, S. Fazzani, R. Tempel, H. Helmboldt, C. Bleschke and A. Kohlmann are employed at LGC GmbH. However, no one at LGC had an influence on the results presented in the manuscript. A. Hagenbach collaborated with LGC for the measurement of crystal structures of compound **5** and **6**.

CRediT authorship contribution statement

Timon Kurzawa: Conceptualization, Investigation, Writing – original draft. **Salim Fazzani:** Investigation. **René Tempel:** Validation. **Hannes Helmboldt:** Validation, Writing – review & editing. **Christian Bleschke:** Supervision. **Andreas Kohlmann:** Project administration. **Adelheid Hagenbach:** Formal analysis, Resources.

Data Availability

The data that has been used is confidential.

Acknowledgement

The analytical department of LGC Luckenwalde is gratefully acknowledged for the measurements of the phenanthridine's analytical data. We thank Dr. F. Beaume for numerous UPLC-MS measurements and A. Bell for proofreading the manuscript.

CCDC 2174442 and 2174443 contains the supplementary crystallographic data for this paper. These data can be obtained free of charge via http://www.ccdc.cam.ac.uk/conts/retrieving.html (or from the Cambridge Crystallographic Data Centre, 12, Union Road, Cambridge CB2 1EZ, UK; fax: +44 1223 336033).

Supplementary materials

Supplementary material associated with this article can be found, in the online version, at doi:10.1016/j.molstruc.2022.134599.

References

[1] A.Y. Abdin, P. Yeboah, C. Jacob, Chemical impurities: an epistemological riddle with serious side effects, Int. J. Environ. Res. Public Health 17 (2020) 1030–1043, doi:10.3390/ijerph17031030.
[2] European Medicines Agency, International Conference on Harmonisation of technical requirements for registration of pharmaceuticals for human use, ICH Q1A(R2), Stability Testing of New Drug Substances and Products. https://www.ema.europa.eu/en/documents/scientific-guideline/ich-q-1-r2-stability-testing-new-drug-substances-products-step-5_en.pdf, 2003 (accessed 23 August 2022).
[3] N.A. McGrath, M. Brichacek, J.T. Njardarson, A graphical journey of innovative organic architectures that have improved our lives, J. Chem. Ed. 87 (2010) 1348–1349, doi:10.1021/ed1003806.
[4] P.A. Thurmann, Valsartan: a novel angiotensin Type 1 receptor antagonist, Expert Opin. Pharmacother. 1 (2000) 337–350, doi:10.1517/14656566.1.2.337.
[5] European Medicines Agency, Update on review of valsartan medicines following detection of impurity in active substance – assessing potential impact on patients is priority. https://www.ema.europa.eu/en/news/update-review-valsartan-medicines-following-detection-impurity-active-substance-assessing-potential, 2018 (accessed 23 August 2022).
[6] D. Ivanovic, A. Malenovic, B. Jancic, M. Medenica, M. Maškovic, Monitoring of impurity level of valsartan and hydrochlorothiazide employing an RP–HPLC gradient mode, J. Liq. Chromatogr. Relat. Technol. 30 (2007) 2879–2890, doi:10.1080/10826070701588638.
[7] B.M. Sudesh, K.S. Uttamrao, Determination and validation of valsartan and its degradation products by isocratic HPLC, J. Chem. Metrol. 3 (2009) 1–12.
[8] A.R. Shrivastava, C.R. Barhate, C.J. Kapadia, Stress degradation studies on Valsartan using validated stability-indicating high-performance thin-layer chromatography, J. Planar Chromatogr. 22 (2009) 411–416, doi:10.1556/jpc.22.2009.6.4.
[9] European Medicines Agency, International Conference on Harmonisation of technical requirements for registration of pharmaceuticals for human use, ICH Q1B Photostability Testing of New Drug Substances and Products. https://www.ema.europa.eu/en/documents/scientific-guideline/ich-q-1-b-photostability-testing-new-active-substances-medicinal-products-step-5_en.pdf, 1998 (accessed 23 August 2022).
[10] V. Agrahari, V. Kabra, S. Gupta, R. Kumar Nema, M. Nagar, C. Karthikeyan, P. Trivedi, Determination of inherent stability of valsartan by stress degradation and its validation by HPLC, Int. J. Pharm. Clin. Res. 1 (2009) 77–81.
[11] K.S. Rao, N. Jena, M.E.B. Rao, Development and validation of a specific stability indicating high performance liquid chromatographic method for Valsartan, J. Young Pharm. 2 (2010) 183–189, doi:10.4103/0975-1483.63166.
[12] K.S. Lakshmi, L. Sivasubramanian, A stability indicating HPLC method for the simultaneous determination of valsartan and ramipril in binary combination, J. Chil. Chem. Soc. 55 (2010) 223–226, doi:10.4067/S0717-97072010000200017.
[13] R.M. Bianchini, P.M. Castellano, T.S. Kaufman, Characterization of two new potential impurities of Valsartan obtained under photodegradation stress condition, J. Pharm. Biomed. Anal. 56 (2011) 16–22, doi:10.1016/j.jpba.2011.04.017.
[14] R.M. Bianchini, P.M. Castellano, T.S. Kaufman, Stress testing of Valsartan. Development and validation of a high performance liquid chromatography stability-indicating assay, J. Liq. Chrom. Rel. Technol. (2012), doi:10.1080/10826076.2011.615094.
[15] S. Mehta, R.P. Shah, S. Singh, Strategy for identification and characterization of small quantities of drug degradation products using LC and LC-MS: application to valsartan, a model drug, Drug Test. Anal. 2 (2010), doi:10.1002/dta.116.

[16] K. Kumaraswamy, H.B. Gandham, R.J.D. Prasad, B.A. Reddy, M. Kaliyaperumal, C.S. Rumalla, Isolation and characterization of novel degradation products of Valsartan by NMR and high resolution mass spectroscopy: development and validation of valsartan by UPLC, Asian J. Chem. 32 (2020) 1064–1068, doi:10.14233/ajchem.2020.22526.
[17] Reaction conditions for the ring contraction of diazirines from tetrazoles in the literature include irradiation in an Ar-matrix at 15 K (17 and 18) and flash vacuum pyrolysis at >400°C (19). Isolation of Diazirine species was not achieved in any of the aforementioned cases: C.M. Nunes, I. Reva, R. Fausto, D. Bégué, C. Wentrup, Bond-shift isomers: the co-existence of allenic and propargylic phenylnitrile imines, Chem. Commun. 51 (2015) 14712–14715, doi:10.1039/C5CC03518J.
[18] C.M. Nunes, I. Reva, M.T.S. Rosado, R. Fausto, The quest for carbenic nitrile imines: experimental and computational characterization of C-amino nitrile imine, Eur. J. Org. Chem. (2015) 7484–7493, doi:10.1002/ejoc.201501153.
[19] D. Begue, G.G.H. Qiao, C. Wentrup, Nitrile imines: matrix isolation, IR spectra, structures, and rearrangement to carbodiimides, J. Am. Chem. Soc. 134 (2012) 5339–5350, doi:10.1021/ja2118442.
[20] Diazirines have been described as photosensitive compounds. In particular, they serve as carbene precursors under irradiation with UV-light for photoreactive crosslinking. For examples see: L. Dubinsky, B.P. Krom, M.M. Meijler, Diazirine based photoaffinity labeling, Bioorg. Med. Chem 20 (2012) 554–570, doi:10.1016/j.bmc.2011.06.066.
[21] J.R. Hill, A.A. Robertson, Fishing for drug targets: A focus on diazirine photoaffinity probe synthesis, J. Med. Chem. 61 (2018) 6945–6963, doi:10.1021/acs.jmedchem.7b01561.
[22] G.M. Sheldrick, A short history of SHELX, Acta Crystallogr. 64 (2008) 112–122, doi:10.1107/S0108767307043930.
[23] G.M. Sheldrick, Crystal structure refinement with SHELXL, Acta Crystallogr. 71 (2015) 3–8, doi:10.1107/S2053229614024218.
[24] Dr.& Dr. H. Putz, K. Brandenburg, Diamond_Crystal and Molecular Structure Visualization Crystal Impact GbR: Bonn, Germany, 2021. Dr.& Dr.version 4.6.5.
[25] J. Zhou, S. Wang, W. Duan, Q. Lina, W. Wei, Catalyst-free photoinduced selective oxidative C(sp3)–C(sp3) bond cleavage in arylamines, Green Chem. 23 (2021) 3261–3267, doi:10.1039/D1GC00743B.
[26] W. Ji, P. Li, S. Yang, L. Wang, Visible-light-induced oxidative formylation of N-alkyl-N-(prop-2-yn-1-yl)anilines with molecular oxygen in the absence of an external photosensitizer, Chem. Commun. 53 (2017) 8482–8485, doi:10.1039/C7CC03693K.
[27] T. Ghosh, A. Das, B. König, Photocatalytic N-formylation of amines via a reductive quenching cycle in the presence of air, Org. Biomol. Chem. 15 (2017) 2536–2540, doi:10.1039/C7OB00250E.
[28] J.B. Roque, Y. Kuroda, L.T. Göttemann, R. Sarpong, Deconstructive fluorination of cyclic amines by carbon-carbon cleavage, Science 361 (2018) 171–174, doi:10.1126/science.aat6365.
[29] J.B. Roque, Y. Kuroda, L.T. Göttemann, R. Sarpong, Deconstructive diversification of cyclic amines, Nature 564 (2018) 244–248, doi:10.1038/s41586-018-0700-3.
[30] J. Genovino, S. Lütz, D. Sames, B.B. Touré, Complementation of biotransformations with chemical C–H oxidation: copper-catalyzed oxidation of tertiary amines in complex pharmaceuticals, J. Am. Chem. Soc. 135 (2013) 12346–12352, doi:10.1021/ja405471h.
[31] W. Li, W. Liu, D.K. Leonard, J. Rabeah, K. Junge, A. Brückner, M. Beller, Practical catalytic cleavage of C(sp3)−C(sp3) bonds in amines, Angew. Chem. Int. Ed. 58 (2019) 10693–10697, doi:10.1002/anie.201903019.
[32] D.K. Leonard, W. Li, K. Junge, M. Beller, Improved bimetallic cobalt–manganese catalysts for selective oxidative cleavage of morpholine derivatives, ACS Catal. 9 (2019) 11125–11129, doi:10.1021/acscatal.9b03476.
[33] Y. He, Z. Zheng, Y. Liu, J. Qiao, X. Zhang, X. Fan, Selective cleavage and tunable functionalization of the C–C/C–N Bonds of N-arylpiperidines promoted by tBuONO, Org. Lett. 21 (2019) 1676–1680, doi:10.1021/acs.orglett.9b00226.
[34] K. He, T. Zhang, S. Zhang, Z. Sun, Y. Zhang, Y. Yuan, X. Jia, Tunable functionalization of saturated C–C and C–H Bonds of N,N′-diarylpiperazines enabled by tert-butyl nitrite (TBN) and $NaNO_2$ systems, Org. Lett. 21 (2019) 5030–5034, doi:10.1021/acs.orglett.9b01574.